A Novel Lithium Ion Battery Autonomous Strategy Improvement Based on SVM-DTC for Urban Electric Vehicle under Several Speeds Tests

Nasri Abdelfatah, Gasbaoui Brahim
Department of electrical engineering, Bechar University, BP417, Bechar 08000, Algeria.
Email: nasriab1978@yahoo.fr, gasbaoui_2009@yahoo.com

Received: July 2011 Revised: August 2011 Accepted: November 2011

ABSTRACT:
Autonomous vehicle present a several problems in the modern commercialized electric vehicle (EV). One of the weakest points of electric vehicles is the battery system, vehicle autonomous depend on the battery state of charge (SOC). In this paper novel strategy of EV power electronics studies based on direct torque space vector modulation technique in the several speed variations .The basic idea of this work that the state SOC equal 70% and the developed model take into consideration the present state under several speed variations. The performances of the proposed strategy controller give a good torque control instead of the speed stability improvement. Moreover, the future industrial's vehicle must take into considerations the obtained results into design steps.

KEYWORDS: Lithium-ion, SOC, SVM-DTC, Electric vehicle.

1. INTRODUCTION

Accuumulator Battery technology is one of most important areas of research for commercial electric vehicles (EVs) used in urban transportation in the present trend and next future. The battery constitutes a very complicated component of the drive train [2,3]. It provides the desired electric power to the traction motor in agreement with the driver's decision. The electrical battery components properties depend on chemical materials and the energy range of this battery for example the battery destined for a bike is different than the battery destined for electric wheel chair. The battery should have a good ability of energy storage, offer high energy efficiency, high current discharge, the capability to charge the empty cells during regenerative braking forces, high cycle life [5, 6]. Many different types of energy storage technologies are under development, batteries are currently used as the main source of electric power in the EV. The three main battery chemistries that find application in the automotive industry are:

- Lead-Acid Battery [1, 2, 3].
- Nickel Metal Hydride Battery.
- Lithium-ion Battery.

State of charge (SOC) symbols the residual capacity of battery and it known as the percent of residual capacity by nominal capacity ,the estimation of SOC of Lithium-ion battery is a key point of energy management system in EV .in order to have a good battery life instead of The autonomous improvement many control are used such as direct torque control based space vector modulation wich's the best solution for torque ripples oscillations [10, 11, 13].The Direct Torque Control strategy (DTC) is one kind of high performance driving technologies for AC motors, due to its simple structure and ability to achieve fast response of flux and torque has attracted growing interest in the recent years. DTC-SVM with PI controller direct torque control without hysteresis band can effectively reduce the torque ripple,the DC-DC converter is use with a control strategy to assure the energy require for the EV and the propulsion system. The aimobject of this paper is to have an idea of the of lithium-ion battery beahvior controlled by DC-DC converter [6,7,8] for utility EV tow rear driving wheel applied direct torque control based space vector modulation under several topology and speed variations.

2. ELECTRIC VEHICLE LOADS DESCIPTION

According to Fig. 1 the opposition forces acting to the vehicle motion are: the rolling resistance force F_{tire} ; the aerodynamic drag force F_{aero} and the climbing force F_{slope} that depends on the road slope [1, 2 , 9].

The global vehicle resistive force is equal to F_r and is the sum of theses resistance forces, as it shown in equation (1).

$$F_r = F_{tire} + F_{aero} + F_{slope} \tag{1}$$

The rolling resistance force is defined by:

$$F_{tire} = mgf_r. \quad (2)$$

The aerodynamic resistance torque is defined as follows:

$$F_{aero} = \frac{1}{2}\rho_{air} A_f C_d v^2 \quad (3)$$

The slope force is usually modeled as:

$$F_{slope} = mg\sin(\beta) \quad (4)$$

where r is the tire radius, m is the vehicle mass, f_r is the rolling resistance force constant, g the gravity acceleration, ρ_{air} is Air density , C_d is the aerodynamic drag coefficient, A_f is the frontal surface area of the vehicle v is the vehicle speed, β is the road slope angle. These parameters values are shown in table1.

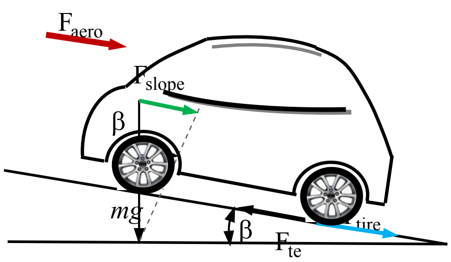

Fig. 1. The forces acting on a vehicle moving along a slope.

Table 1. Parameters of the electric vehicle model

r	0.32 m	A_f	2.60 m^2
m	1300 Kg	C_d	0.32
f_r	0.01	ρ_{air}	1.2 Kg/m^3

The vehicle considered in this work is two-rear-driving wheels of EV destined for urban transportation. Two induction motors are coupled in each of the rear wheels. The energy source of the electric motors ensured by the Lithium-ion battery controlled by Buck boost DC-DC converter [4,5,6,8].The EV control propulsion system schema is shown in Fig. 5. The differential electronics gives the necessary reference speed of each wheels in right and curved road toplogies [2,9].

3. LITHIUM- IONS BATTERY DESCRIPTION

Lithium-ion batteries are rechargeable batteries, where lithium-ion moves from anode to cathode to charge and discharge the battery. Lithium-ion batteries are available in a variety of utilizations and variety of materials that have unique cost, performance, and aging characteristics [7,14, 15].The chemistry reaction in the discharge phase are defined by equation (5) and (6).

$$LiC_6 \Leftrightarrow Li^+ + e^- + C_6 \quad (5)$$

$$Li^+ + e^- + Co_2 \Leftrightarrow LiCoO_2 \quad (6)$$

As illustrated in Fig. 2, lithium-ion batteries are comprised of an anode, cathode, separator, and some form of electrolyte. There are four classes of anodes in lithium-ion batteries: alloys/intermetallics, oxides, lithium metals, but typically are made of some type of carbon. The separator is normally a semi-permeable plastic that allows lithium ions to pass through but prevents a short circuit between the anode and cathode. The electrolyte in a Lithium-ion battery can be an organic liquid solvent, polymer, gels, or an ionic liquid but all the materials act as a carrier to conduct lithium ions between the anode and cathode.

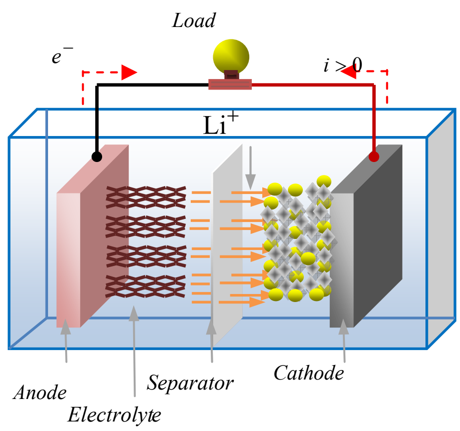

Fig. 2. Lithium-ion battery discharge diagram.

$$Li^+ + e^- + C_6 \Leftrightarrow LiC6 \quad (7)$$

$$LiCoO_2 \Leftrightarrow Li^+ + e^- + Co_2 \quad (8)$$

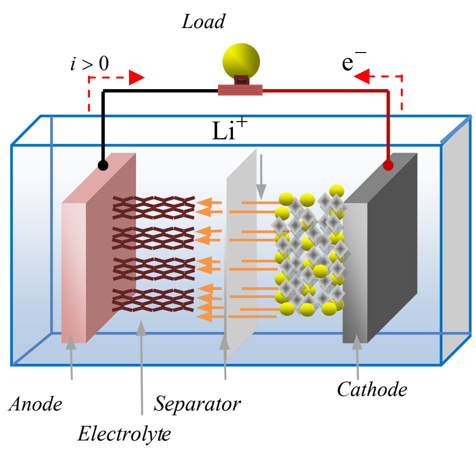

Fig. 3. Lithium-ion battery charge diagram.

When the anode and cathode are connected to a charger, as it illustrated in Fig. 3, the electrodes undergo a reduction-oxidation reaction. In the cathode oxidation occur causing electrons to be lost (increase oxidation state) and take an external path to the anode. The lithium-ions from the cathode are conducted by the electrolyte through the separator to the anode. The anode gains the electrons from the cathode in a process called reduction (decrease oxidation state[1,2,7]. During a discharge the process is reversed where the cathode gains electrons and the lithium-ions pass from the anode to the cathode. Cell capacities are measured in amp hours (Ah) and the C-rate in batteries refer to the batteries ability to supply current as a multiple of the cell's capacity [14, 15]. The chemistry reaction in the charge phase are defined by equation (7) and (8).

Fig 4. describe the equivalent circuit of Lithium-ion battery[1,2,3,7] where, E is the no load voltage , E_0 is the constant voltage, K is the polarization constant resistance's, Q is maximum battery capacity, Q is exponential voltage , B is exponential capacity.

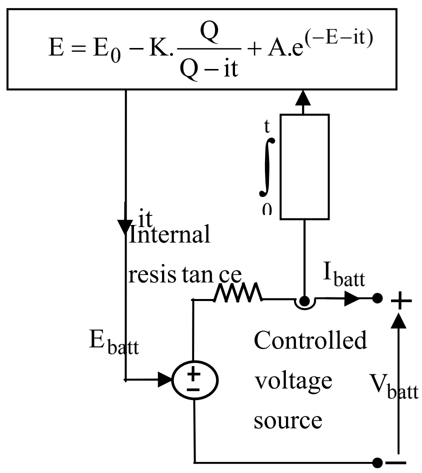

Fig. 4. The equivalent circuit of Lithium-ion battery.

The State-Of-Charge (SOC) of the battery takes value (between 0 and 100%). The SOC for a fully charged battery is 100% and for an empty battery is 0%. The SOC can be defined by equation (9):

$$SOC = 100\left(1 - \frac{Q.1.05}{\int i.dt}\right) \tag{9}$$

The Lithium-ion battery parameters are illustrate in table2 as follow:

Table 2. Lithium-ion parameter

Rated capacity	6.5 Ah
Nominal Voltage	1.18 V
Maximum Capacity	7 Ah
Nominal Discharge Current	1.3 A
Exponential Voltage	1.28 V
Internal Resistance	2 mΩ
Rated Capacity	6.5 Ah
Fully Charged voltage	1.39 V
Capacity Nominal Voltage	6.25 Ah
Exponential Capacity	1.3 Ah
Exponentiel Voltage	1.28 V

4. DIRECT TORQUE CONTROL STRATEGY BASED SPACE VECTOR MODULATION (SVM-DTC)

This technique consist of two proportional integral (PI) classical controllers regulating the torque and the flux magnitude instead of hysteresis band as it shown in Fig.5, by generating the voltage signs for inverter control. Noting that no decoupling mechanism is required for the torque and magnitude flux controls. Due to the structure of the inverter, the DC bus voltage is fixed, the speed of speed of voltage space vectors is adjusted by the using of the zero voltage vectors to control the electromagnetic torque generated by the induction motor, the selection of voltage vectors is also changed, Its not based on the flux linkage region, but on the error vector between the expected and the estimated flux linkage [10, 11,12, 13]. The induction motor stator flux can be estimated by:

$$\phi_{ds} = \int_0^t (V_{ds} - R_s i_{ds})dt \tag{10}$$

$$\phi_{qs} = \int_0^t (V_{qs} - R_s i_{qs})dt \tag{11}$$

$$|\phi_s| = \sqrt{\phi_{ds}^2 + \phi_{qs}^2} \tag{12}$$

$$\theta_s = \tan^{-1}\left(\frac{\phi_{qs}}{\phi_{ds}}\right) \tag{13}$$

The electromagnetic torque T_{em} can be given as follow:

$$T_{em} = \frac{3}{2} p(\phi_{ds} i_{qs} - \phi_{qs} i_{ds}) \tag{14}$$

The SVM principle is based on the switching between two adjacent active vectors and two zero vectors during one switching period. It uses the space vector concept to compute the duty cycle of the switches.

5. BUCK BOOST DC-DC CONVERTER FOR ELECTRIC VEHICLE

Buck boosts DC-DC converters help the battery charging in regenerative braking phases where the backup power are required in order to maintain the necessary storage for the specific trajectory . The power flow is moved in a bidirectional trajectories [4, 5].An EV buck boost converter provides an output voltage which can be higher or lower than the battery input voltage [5, 6,8].

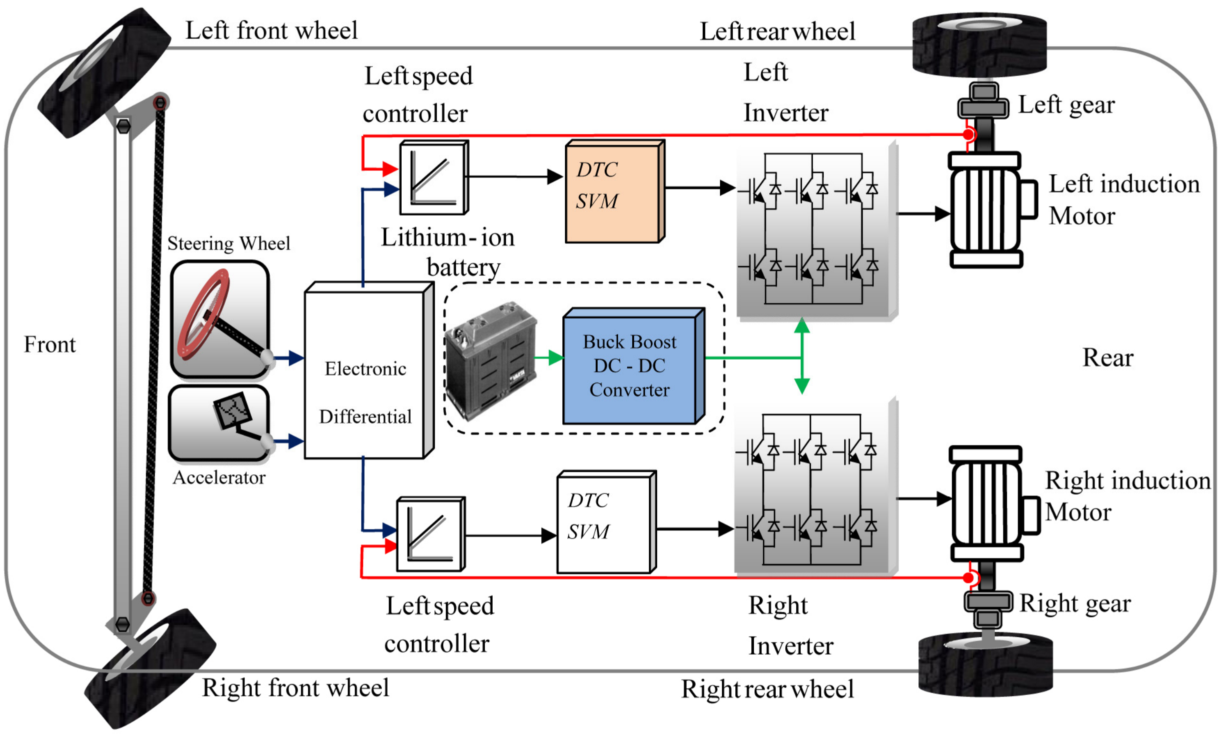

Fig. 5. The driving wheels control system

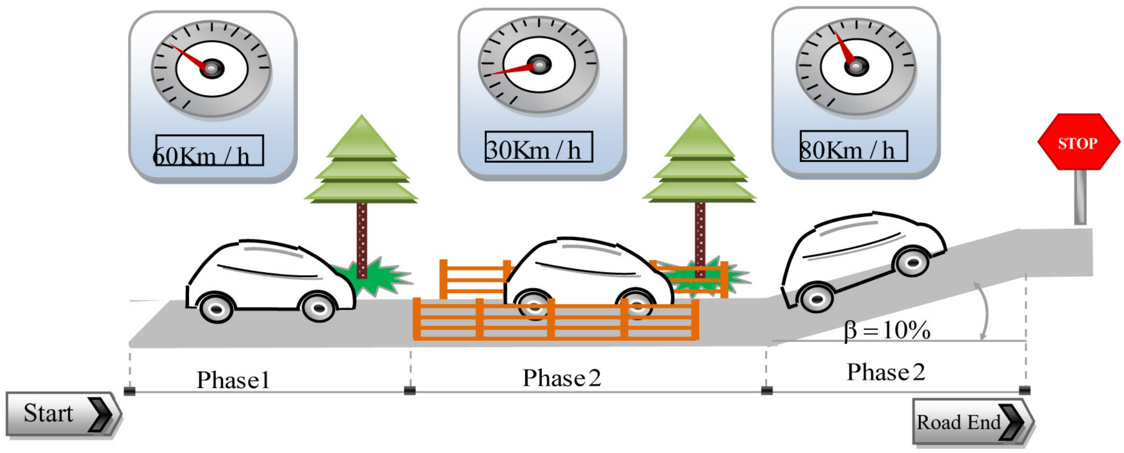

Fig.6. Specific driving road topologies

6. SIMULATION RESULTS

In order to characterize the driving wheel system behavior, simulations were carried using the model of Fig 5 and the specefic road shema of Fig.6.The following results were simulated in MATLAB .

The topology studied in this present work consists of three phases: the first one represent the acceleration phase's beginning with 60 Km/h in straight road, the second phase represent the deceleration one when the speed became 30 Km/h, and finally the EV is moving up the slopped road of 10% under 80 Km/h, the assumption that the initialized lithium-ion battery SOC is equal to 70% during simulations the specified road topology is shown in Fig. 6, when the speed road constraints are described in the table 3.

Table 3. Specified driving route topology

Phases	Event information	Vehicle Speed [km/h]
1	Acceleration	60
2	Bridge, Break	30
3	Acceleration and climbing a slope 10%	80

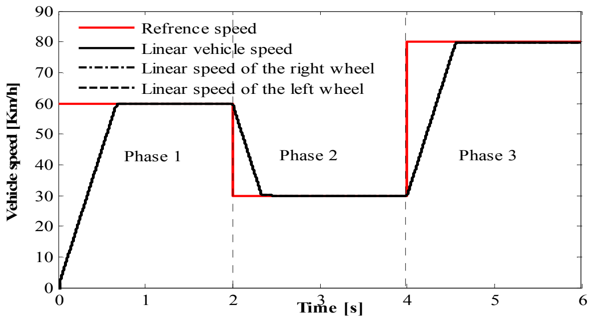

Fig. 7. Variation of vehicle speeds in different phases

Refereed to Fig.7 at time of 2sec the vehicle driver move on straight road with linear speed of 60 km/h, the assumption's that the two motors are not disturbed and the initial SOC of 70 % is respected. In this case the driving wheels follow the same path with no overshoot and without error which can be justified with the good electronic differential act coupled with DTC-SVM performances.

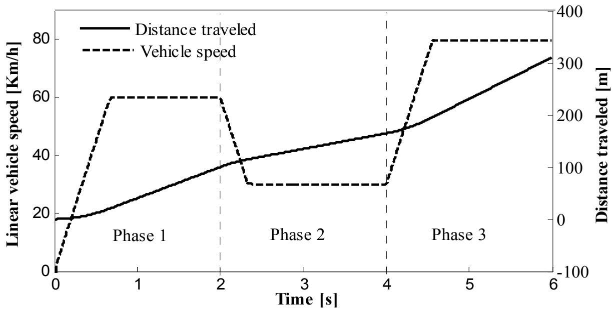

Fig. 8. Evaluation of vehicle and distance travelled in different phases

Fig.8 reflect the relationship between vehicle speed's variation and distance traveled in different phases. The distance travelled of 310 m in three electronic differential references speeds actions : from 60km/h then hard break until the value of 30km/h and the acceleration phase until the speed of 80km/h .

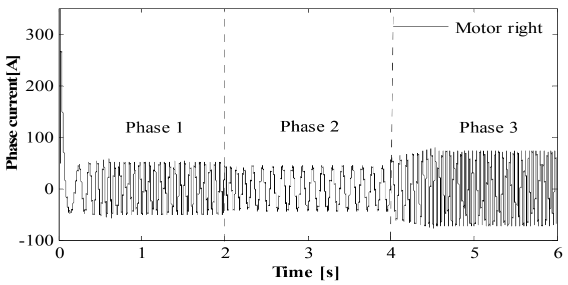

Fig. 9. Variation of phase current of the right motor in different phases.

Figures 9 and 10 and table 4 explains the variation of phase current and driving force respectively. In the first step and to reach 60 km/h The EV demand a current of 50.70 A for each motor which explained with driving force of 329.30N. In second phase the current and driving forces demand decrees by means that the vehicle is in recharging phase's which explained with the decreasing of current demand and developed driving forces shown in Figures 9 and 10 respectively. The last phases explain the effect of acceleration under the slope on the straight road EV moving. The driving wheels forces increase and the current demand undergo double of the current braking phases the battery use 80 % of his power to satisfy the motorization demand under the slopped road condition which is explained by the development of the globally vehicle resistive torque illustrate in Fig.11. In the other hand the linear speeds of the two induction motors stay the same and the road slope does not influence the torque control of each wheels. The results are listed in table 4.

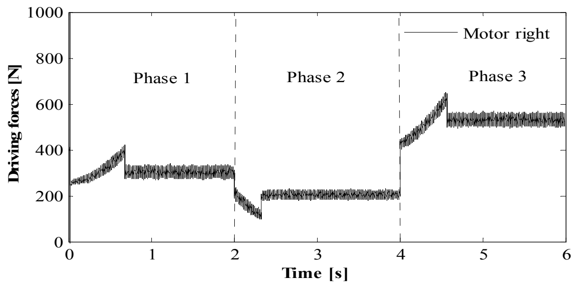

Fig. 10. Variation of driving force of the right motor in different phases

Table 4. Values of phase current driving force of the right motor in different phases

Phases	Phase 1	Phase 2	Phase 3
Current of the right motor [A]	50.71	44.21	70.78
Driving force of the right motor [N]	329.30	228.50	563.00

According to the table 4 and and table 5, we say that: the vehicle resistive torque was 95.31 N.m in the first case (acceleration phase) when the power propulsion system resistive one is only 68.53 Nm in the breaking phases (phases 2) , the back driving wheels develop more and more efforts to satisfy the traction chain demand which corresonding to an resistive torque of 168.00 N.m .The result prove that the traction chain under acceleration demand develop the double effort comparing with the breaking phase case's ,by means that the vehicle needs the half of its energy in the deceleration phase's compared with the acceleration one's as it specified in table. 5 and Fig .11.

Table 5. Variation of vehicle torque in different Phases

Phases	1	2	3
the Vehicle resistive torque [N.m]	95.31	68.53	168.00
the globally vehicle resistive torque in Percent	20.02 %	14.39 %	35.29 %

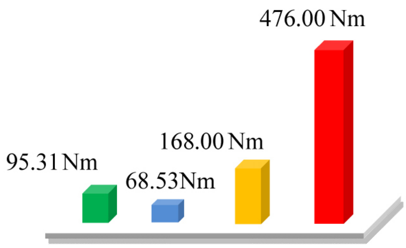

Fig.11. Evaluation of the globally vehicle resistive torque compared to nominal motor torque in different phases

7. CONCLUSIONS

The vehicle energy policy outlined in this paper has demonstrated that the lithium-ion battery behavior controlled by buck boost DC-DC converter can be improved using direct torque control strategy based on space vector modulation and used for the next future utility EV which utilize tow rear driving wheel for motion, where the battery developed power depend on the speed reference of the driver. The several speed variations do not affect the performances of the buck boost DC-DC converter and the control strategy gives good dynamic characteristics of the EV propulsion system.

8. APPENDIX

Table 6. Induction motors parameters

Rr	Rotor winding résistance	0.0503
Rs	Stator winding résistance	0.08233
Ls	Stator leakage inductance	0.000724
Lmm	Magnetizing inductance	0.02711
Lr	Rotor leakage inductance	0.000724
fc	Friction coefficient	0.0014
P	Number of pôles	4

REFERENCES

[1] M.Salman, M.Chang, J.Chen, **"Predictive energy management strategies for hybrid vehicles"**, *IEEE VPPC, Chicago, IL*, Sep. 7–9, pp. 21–25, 2005.

[2] J.Larminie, J.Lowry, **"Electric Vehicle Technology Explained"**, *Edited by John Wiley and John Lowry*, England, 2003.

[3] R.F.Nelson, **"Power requirements for battery in HEVs"**, *J. Power Sources*, Vol. 91, pp. 2–26, 2000.

[4] C.Xia, Y.Guo, **"Implementation of a Bi-directional DC/DC Converter in the Electric Vehicle"**, *Journal of Power Electronics*, Vol. 40, no. 1, pp. 70–72, 2006.

[5] Q.Zhang, Y.Yin, **"Analysis and Evaluation of Bidirectional DC/DC Converter"**, *Journal of Power Technology,* Vol. 1, no. 4, pp. 331–338, 2003

[6] S.Buso, **"Design of Robust Voltage Controller for a Buck-Boost Converter Using µ-Synthesis, "** *IEEE Transactions on Control Systems Technology*. Vol. 7, no. 2, pp. 222–229, 1999.

[7] X.X.Yan, D.Patterson, **"Novel power management for high performance and cost reduction in an electric vehicle"**, *Renew. Energy*, 22, (1–3), pp. 177–183, 2001.

[8] H.J.Chill, L.W. Lin, **"A Bidirectional DC-DC Converter for Fuel Cell Electric Vehicle Driving System"**, *IEEE Trans. Power Electron*, Vol. 21, pp. 950–958, 2006.

[9] A.Nasri,A.Hazzab, I.K.Bousserhane,S.Hadjeri,P.Sicard, **"Fuzzy logic Speed control stability improvement of lightweight electric vehicle drive"** *Journal of electrical engineering b & Technology* Vol. 5, No. 1, pp. 129~139, 2010..

[10] M. E. H. Benbouzid et al., **"Advanced fault-tolerant control of inductionmotor drives for EV/HEV traction applications: From conventional to modern and intelligent control techniques,"** *IEEE Trans. Veh. Technol.,* Vol. 56, no. 2, pp. 519–528, Mar. 2007.

[11] A. Gupta, A. M. Khambadkone **"A space vector pwm scheme for multilevel inverters based on two-level space vector pwm,"** *IEEE Transaction on Industrial Electronics,* Vol. 53, October 2006.

[12] T. G. Habetler, F. Profumo, M.Pastorelli, L. Tolbert **"Direct torque control of induction machines using space vector modulation,"** *IEEE Transaction on Industry Applications*, Vol. 28, no. 5, pp. 1045-1053, septembre/October 1992.

[13] SUN Dan, HE Yi-kang. **"Space vector modulated based constant switching frequency direct torque control for permanent magnet synchronous motor"**. *Proceedings of the CSEE*, 2005, 25(12): 112- 116.

[14] Guidi, Giuseppe., Energy Management Systems on Board of Electric Vehicles, Based on Power Electronics. Trondheim : Norwegian University of Science and Technology, 2009.

[15] Zhang, D, et al., **"Studies on capacity fade of lithium-ion batteries. "** *Journal of Power Sources, 2000*, Vol. 91, pp. 122 - 129. 0378-7753.